Editors: **Singhroy**, Vern (Ed.)

Provides case studies of practical and advanced methods using satellite images to monitor infrastructure

Discusses the applications and limitations of satellite images for infrastructure in an international context

Focuses on urban and rural centers, mines, oil platforms, and transportation and energy infrastructures

About this book | About the authors

Dr Vernon Singhroy is the President of EOSPATIAL in Ottawa, Canada. He is an internationally recognized expert on remote sensing applications, and was the chief scientist of the Canadian Space Agency, RADARSAT Constellation Mission, launched in June 2019. Dr. Singhroy received his Ph.D. in environmental and resource engineering from the State University of New York, Syracuse. He is a professional engineer. A senior research scientist with the Canada Centre for Remote Sensing at Natural Resources Canada (1995-2020), Dr. Singhroy has published over 300 papers in scientific journals, proceedings, and books. He was the editor-in-chief of the Canadian Journal of Remote Sensing, and he is the co-editor of four books, including of the Encyclopedia of Remote Sensing. Dr. Singhroy has been a Professor of Earth Observation at the International Space University in Strasbourg, France (1998-2020) and he is an adjunct professor in Planetary and Space Sciences at the University of New Brunswick in Canada. Dr. Singhroy received the prestigious Gold Medal Award from the Canadian Remote Sensing Society and the Queen Elizabeth Diamond Jubilee Medal for his contributions to Canadian and international remote sensing applications and education.

Advances in Remote Sensing for Infrastructure Monitoring

Advanced radar images for monitoring Transportation, Energy, Mining and Coastal Infrastructure

Vernon Singhroy et al.

vern.singhroy@eospatial.com

Abstract

This paper provides a summary of the most current sensors being used for monitoring infrastructure. We also provide case studies on:

- The use of time-series radar interferometry (InSAR) to monitor critical highways, railways, and pipelines affected by landslides that are triggered by coastal erosion, spring snow melt, permafrost thaw, monsoons and hurricanes.
- The use of InSAR, change detection, and image fusion techniques to explore and monitor mining sites.
- The use of radar images to monitor shoreline change and oil spills.

We have shown that high-resolution InSAR images are effective as an early warning system to monitor:

- Landslides along highways and railways in coastal and mountainous areas.
- Safe mining practices and heaving rates produced by steam injection in the mining of the oil sands.
- Pipeline corridors in high risk mountainous, wetlands, and permafrost terrains to prevent oil spills.

We have also shown that radar time-series, change detection and polarmetric image fusion techniques are effective to identify

- mining practice and illegal mining in cloudy remote tropical areas.
- shifting low lying coastlines caused by rising sea level affecting coastal infrastructure.
- faults to improve mineral exploration
- oil spills from ocean drilling platforms

These case studies will assist in providing guidelines for the use of advanced radar image techniques for monitoring infrastructure related to civil engineering construction and mining.

Keywords: Infrastructure monitoring, high-resolution InSAR, transportation and energy corridors, oil extraction, oil spills, mining.

1: Introduction

In this book we focus on the use of advanced radar imaging techniques to monitor some of the main types of critical transportation and energy infrastructure, such as roads, railways, and pipelines. We provide case studies on mining infrastructure to locate and monitor active mining sites. Imaging techniques used to facilitate mineral exploration are discussed. Radar monitoring techniques for shoreline change and ocean oil spills affecting coastal infrastructure, are also included. These operational examples will assist in providing guidelines on the use of advanced radar imaging techniques to characterize and monitor civil infrastructure. They will also be useful in the planning of future sustainable climate resilient infrastructure (InterAmerican Development Bank 18).

InSAR Infrastructure

Monitoring surface deformation on civil infrastructures requires high resolution, spatial, and temporal InSAR imagery for mitigation and safety purposes. An interferometric image represents the phase difference between the backscattered signals of two SAR images obtained from similar positions in space. In the case of space borne SAR, the images are acquired from repeat-pass orbits. The phase differences result from topography and changes in the line-of-sight distance (range) to the radar due to surface displacement, or changes in the atmospheric propagation path length. Typical scales for SAR interferometry in land deformation applications are millimeters to centimeters per orbit cycle of the radar satellite.

Radar interferometry (InSAR) techniques that use imagery from several radar satellites are increasingly being used for deformation monitoring (Singhroy et al., 2005; 2008; 2016; Colesani and Wasowski, 2006; Singhroy, 2008; 2010; Calò et al., 2012; 2014; Wasowski and Bovenga, 2014a& b, and others). In some cases, ground-based InSAR data (Pratesi et al., 2015) are being used, but these are not discussed in this book. Our examples demonstrate the operational use of space-based InSAR for infrastructure. The application of InSAR techniques to monitor unstable slopes in both rock and soil has been developing rapidly, including its application to other deformation studies, such as subsidence, volcanoes, and earthquakes.

Landslides affecting infrastructure can result in extreme economic and societal costs, despite our increased understanding of the mechanisms of failure and large ground deformation (Singhroy, 2012). Current state of the art, real-time monitoring of active slopes developed for early warning of landslides is very expensive. Radar interferometry is increasingly being used to complement real-time monitoring techniques such as GPS and in situ field measurements (Singhroy and Molch, 2004; Singhroy, 2005; Alasset et al.,2007; Pearce et al., 2014).

Other case studies in this chapter use standard operational image processing techniques. These include multi-date radar change detection to monitor shoreline changes and update mining sites. Enhanced image visualization and filtering was also used for ocean oil spill detection.

Sensors for Infrastructure

This section is written for folks with little knowledge of remote sensing applications. We therefore summarize some relevant information related to infrastructure. Tables 1 and 2 provide the specifications and applications of the current and upcoming radar satellites. Table 3 provides a list of the current radar and optical sensors that can be used to characterize and monitor transportation, energy, and mining infrastructure. This introduction is a background to support the images and techniques related to the case studies described in this chapter.

RADAR is an acronym for **RA**dio **D**etection **A**nd **R**anging, which essentially characterizes the function and operation of a radar sensor. The sensor installed on airplanes and satellites transmits a microwave (radio) signal towards the target on Earth and receives the backscattered portion of the signal. The strength of the backscattered signal is measured to discriminate between different targets.

Operational applications of radar imagery have been developed over the past thirty years. Currently, radar satellites provide high-resolution (1-10 m) and medium to low resolution (10-100 m), day-and-night, all-weather imagery for many research applications. These include geoscience and climate change research, environmental and disaster monitoring, topographic mapping, change detection, security-related applications, and planetary exploration (Moreira et al., 2013; Singhroy, 2013). Table 1 provides a summary of current and future radar satellite missions, and their technical specifications. The major space agencies focused on launching C-, X-, S-, and L-band frequency satellites with different resolutions, viewing geometries, and polarizations.

There are a number of high-resolution radar constellation satellites being planned (Table 1). For example, the recently launched (June 2019) RADARSAT Constellation Mission (RCM) is designed as a scalable constellation of three small satellites. RCM is optimized for coherent change detection (CCD), a compact polarimetry mode (Charbonneau, 2010), special imaging modes optimized for ship detection, and a combined SAR and automatic identification system (AIS) (Thompson, 2015). The frequent revisits of RCM will allow 1 day global monitoring for applications such as maritime surveillance, disaster management, and ecosystem monitoring.

Table 2 provides a summary and the ratings for the overall applications of RADARSAT-1 & 2 and the potential applications of the RADARSAT Constellation Mission. Other radar satellites can provide similar applications.

RADARSAT-2 has improved multipolarization and higher resolution capabilities in comparison to RADARSAT-1 and ENVISAT. This improvement has allowed for further developments in agricultural applications, particularly crop-type mapping and condition assessment, soil tillage and crop residue mapping, and soil moisture estimation. The additional polarizations have increased the information and understanding of the scattering mechanisms and target interactions. Integrating C-band SAR with other radar frequencies, or with data acquired by optical sensors, has provided many operational applications (McNarin and Brisco, 2004; Singhroy and Pilkington, 2012 among others).

SAR polarimetry is a widely used technique to derive qualitative and quantitative physical information for land and water. This is based on the measurement of the polarimetric signatures of natural, agricultural, and man-made scatterers. The scattering mechanism allows for their identification and separation, and are based on the shape, orientation and dielectric properties of the target (Cloude, 2010; Moreira et al., 2013; Lopez-Sanchez et al., 2014). For example, the RADARSAT Constellation Mission (RCM) consists of three small synthetic aperture radar (SAR) satellites flying in a constellation configuration. It has fully polarimetric (FP) capabilities, in addition to single-polarization (HH, HV, VV), conventional (HH-HV, VV-VH, and HH-VV), and hybrid (i.e., compact) dual polarization. Recent results have shown that the multi-frequency and compact polarimetric images from RCM, when combined with fully polarimetric data, were useful for estimating soil moisture conditions, and improved ship detection and classification, and the mapping of geological structures (Merzouki and McNairn, 2015; Touzi and Vachon, 2015; Fobert et al., 2018).

Radar interferometry (InSAR) represents the phase differences between the backscatter signals in two or more time-series SAR images obtained from similar positions in space. Radar satellites acquire images from repeat-pass orbits. These orbit cycles, from current radar satellites, can range from 1- 6 days for Cosmo-SkyMed, 4 days for RCM, 11 days for TerraSAR-X, and 12 days for Sentinel-1. Table 1 provides a summary of the technical specifications of these satellites.

The phase differences between two repeat-pass images at a fixed line of site (LOS) can provide information on topography, small surface displacements, or changes in the atmospheric propagation path length. Land deformation measured from SAR interferometry ranges from millimeters to centimeters per orbit cycle. InSAR techniques are used to monitor deformation under specific conditions, provided that coherence is maintained over the respective orbit cycle. Using data pairs with short perpendicular baselines, short time intervals between acquisitions, and correcting for the effect of topography and atmospheric effects, reliable measurements of surface deformation can be achieved.

InSAR techniques using images from several radar satellites are increasingly being used for landslide deformation monitoring (Colesani and Wasowski, 2006; Singhroy, 2012; Calo et al., 2014; Singhroy et al.,2016; Bianchini et al., 2018). InSAR can assist in characterizing and monitoring geohazards, and can be used as a screening tool for mitigation and remediation for the protection of assets, property, and life (Singhroy, 2017; Gee et al., 2019). InSAR techniques are also being used to monitor co-seismic deformation (Boncori, 2019), volcanic eruption (Dumont et al., 2018 and others), and glacier retreat (Brancato et al., 2020 and others). Some examples are described below as they relate to infrastructure monitoring.

Optical:

Table 3 provides a summary of the capabilities of other imaging sensors for mapping and monitoring infrastructure.

Optical images use the visible, near infrared, and short wave infrared parts of the electromagnetic spectrum. The images are acquired from aircraft and satellites. Aerial photos are still being used for mapping and interpreting landforms and surficial materials related to civil engineering work. All civil construction is built on solid bedrock and surficial soil materials, therefore, knowing their distribution and properties are fundamental. Mollard and Janes (1983) provided useful keys and examples of air photo interpretation for various terrain and surficial materials that can be used for transportation, energy corridor, and mining infrastructure. Table 3 summarizes some of the ways air photos are applied for mapping attributes for infrastructure.

High-resolution optical systems (0.5-5 m spatial resolution) are generally the most useful in identifying and interpreting the fine details required for monitoring civil engineering work. Table 3 provides a summary of the capabilities of high-resolution optical sensors for infrastructure. Several case studies on the use of high-resolution optical images, and other spatial data related to monitoring infrastructure and site characterization, are described in this book and by Singhroy (1996).

Hyperspectral images provide high spatial and spectral information that are particularly useful in infrastructure site characterization, geological mapping, and mineral exploration. They can provide sub-pixel compositional information to identify surface minerals of exposed rocks. Spectral libraries and image enhancement techniques are now used in mineral identification, mine tailings and oil contamination sites as part of the techniques associated with mining infrastructure (Singhroy, 1996; van der Meer et al., 2012; Del'Papa Moreira Scafutto et al., 2016). Spectral signatures from field and airborne sensors were also used to identify surface mineralization and stressed vegetation associated with high concentrations of base metals in the surficial material (Singhroy and Kruse, 1999; Feng et al., 2018).

The occurrence of oil spills indicate damage to the pipelines. Finding these on-land spills can guide cleanup and repair operations. Hyperspectral images were used to characterize the type of oil contamination in mine tailings (Del'Papa Moreira Scafutto et al., 2016).

UAV

Unmanned aerial vehicle (UAV) systems are generally understood as drones with RGB cameras. Current UAV systems are providing multispectral, hyperspectral, longwave infrared range cameras (thermal) and light-weight LiDAR (light detection and ranging) data (Yao et al., 2019). UAV sensors and platforms are used for Structural Health Monitoring (SHM) related to the integrity of engineering structures. Research has shown that UAVs are increasingly being used to monitor infrastructure for early warning, situational assessment, and decision support applications (Flammini et al., 2016). The short response time and low mobility cost of UAVs will be useful for monitoring civil engineering works. These high-resolution drone images are also used in several other applications, such as agriculture, forestry, mining, and environmental, among others

(Fernandes et al., 2018; Yao et al., 2019; Poley and McDermid, 2020). Drone images will continue to provide a powerful tool for infrastructure monitoring because of their ultra high spatial resolution, flexibility, and ease of integration with other high-resolution radar, LiDAR and optical images. Table 3 provides some of the applications of drone images for infrastructure monitoring and characterization.

LIDAR

Light Detection And Ranging (LiDAR) provides accurate three-dimensional (3D) point cloud data that are used to characterize, monitor, and plan civil infrastructure developments. LiDAR is used for topographic mapping because of its capability to provide 3D measurements. As the light wave passes through the vegetation, the backscatter wave provides information about the vegetation parameters. Airborne Laser Scanning (ALS) are mainly used to generate detailed bare earth digital terrain models (DTM) and to estimate forest height, density, etc. ALS systems emit laser pulses with footprints ranging from 0.1 m to 2 m near the surface for submeter measurement accuracy of the terrain surface height (White et al., 2016; Shang et al., 2019). Terrestrial Laser Scanners (TLS) and Mobile Laser Scanning (MLS) provide millimeter-level accuracy and have point densities of a few thousand points/m2. MLS has many applications, including the monitoring of urban transportation infrastructure (Wang et al., 2019; Sánchez-Rodríguez, 2019). TLSs are used for measuring and monitoring specific infrastructure and buildings with high levels of detail (e.g., Nowak et al., 2020). Multispectral laser scanning is a rapidly growing technology. Images are acquired at different wavelengths allowing for the recording of a diversity of spectral reflectance. The multispectral LiDAR data, using intensity and height images created from LiDAR points, provide detailed land cover classification in urban environments (Morsy et al., 2017). Table 2 shows some of the main application of lidar data for measuring attributes related to civil infrastructure.

2: Transportation Corridors

2.1 InSAR monitoring of a major highway affected by coastal landslide

Canada has the longest coastline in the world. Coastal hazards are frequent because of various combinations of topographic, geomorphic, and geological conditions, which are conducive to mass failure (Mosher, 2008). In addition, the stability of the coastal environment is impacted by climatic, geographic, oceanographic and anthropogenic factors (Irvine, 2012). Coastal landslides represent a specific threat on the coastlines of populated areas in southern British Columbia and the Atlantic provinces because of the high tsunami potential. These landslides are triggered by seawater intrusion, coastal scouring, high intensity/frequency rainfall and storm events, human activity, and rapid snowmelt. They are aided by favourable geological and geotechnical conditions, such as fractured bedrock on steep slopes or earthquake tremors. They usually occur without warning and with little time lag between failures. Therefore, high resolution, spatial, and rapid temporal images generated from the RADARSAT Constellation Mission are required as part of the integrated monitoring of these coastlines.

We acquired RADARSAT-2 InSAR images in ultra-fine beam mode (U17, ~3 m resolution) with 43° incidence angle and HH polarization for every 24 day orbital cycle from March to October

2010. During the summer of 2010, we acquired TerraSAR-X InSAR images every 11 days for three months to fill the gaps between the RADARSAT-2 acquisitions. The TerraSAR-X data were in spotlight (1 m) mode with 43.1° incidence angle and HH polarization.

Our InSAR method used the GAMMA software to perform standard interferometric processing (Gamma Remote Sensing, 2015). This includes image co-registration and re-sampling, interferogram generation, topographic phase removal using a 1 m Lidar DEM to get a set of co-registered unwrapped differential interferograms for both RADARSAT-2 and TerraSAR-X data. An improved SBAS (Small Baseline Subset) algorithm (Samsonov et al., 2011) was applied to the unwrapped differential interferograms. The SBAS method minimizes the effects of the atmosphere and the lack of resolution in the DEM on the accuracy of InSAR measurements. It produces a deformation time-series using interferograms with short time acquisitions, which are usually more coherent. A high-pass filter with a Gaussian window was applied to remove the residual orbital and long wavelength atmospheric signals. A Singular Value Decomposition (SVD) inversion was applied to simultaneously solve for the individual deformation rates and the residual topographic errors.

During the spring of 2008, the coastal landslide at Daniel's Harbour destroyed several homes, as well as the only highway corridor connecting all the settlements along the northeastern coast. After the event, the wet landslide debris continued to move about 25 mm during the summer and early fall months, as shown in Figure 1.

Our field investigation and earlier geotechnical investigations by Batterson et al. (1999) suggested that the Daniel's Harbour landslide was triggered by coastal erosion from high winter ocean waves combined with spring rainfall and groundwater seeps from the nearby reservoir. In other coastal areas of Newfoundland, sea-level rise, wave action, slope angle, sediment type, storm surge and human activities are the main factors triggering landslides (Irvine, 2012). The high-resolution InSAR images are effective in characterizing differential motion on this coastal landslide, especially during active wet spring periods. Because these are spontaneous events, a four day revisit from RCM will provide an improvement to current RADARSAT-2, Sentinel-1, TerraSAR-X, and ALOS-2 acquisitions over the active spring and summer months in these coastal areas. In the tropical areas, similar methods can be applied during the hurricane and typhoon seasons.

2.2 InSAR monitoring of a coastal railway

This case study reports on a rock failure affecting a nearby railway line. Field measurements of fissures show crack widths of tens of centimeters to meters, which indicate significant rock slope movement (Locat et al., 2010). We use InSAR techniques to monitor rock slope movement as part of a continuous monitoring program. Our results show 30 mm of motion using RADARSAT-2 images over a 2 year period.

The site is highly vegetated with mature trees which strongly reduces the InSAR coherence at C-band. We installed twenty-three metallic reflectors (13 trihedrals and 10 dihedrals) within and outside the landslide area to monitor the landslide motion. The reflectors serve as permanent coherent targets with high backscattering intensity and accurate phase (Figure 2). The locations of

the reflectors within and outside the landslide area were based on prior knowledge of the unstable rock slope.

Seven targets are oriented and inclined to maximize the line of sight (LOS) backscattering return of RADARSAT-2 Spotlight (SLA3, at $\theta = 32^{o}$) for ascending passes. Sixteen targets are oriented for descending passes and inclined to optimize the return for RADARSAT-2 Spotlight SLA 76 and SLA19 ($\theta = 27^{o}$ and 44^{o} respectively).

Our InSAR displacement estimates show that the landslide is characterized by a more complex series of active blocks than previously estimated from traditional in situ instruments. All these blocks are moving at different rates, from 15 to 55 mm a year, as shown in Figure 3. Results from ground-based monitoring instrumentation confirmed our displacement measurements and have assisted in the understanding of the failure mechanisms of this complex rockslide (Cloutier et al., 2010).

At the Gascons site, we observed that a combination of favourable geological conditions, combined with fractured bedrock, produced multiple failure mechanisms which require high-resolution rapid monitoring throughout the year. High-resolution data, and the 4 day repeat pass provided by the RADARSAT Constellation Mission, would maintain high coherence and detailed resolution to monitor the moving blocks within the rock slide.

2.4 InSAR monitoring of a Himalayan highway and railway affected by Monsoons

In this study, we used RADARSAT-2 InSAR to assist in developing an early warning system for Himalayan landslides. In Darjeeling district, West Bengal, there are about 3000 landslides, many of which are active and retrogressive. They are affecting settlements and transportation corridors, and in some cases, have caused fatalities (Ghosh et al., 2011; Das et al., 2018). The movement of these landslides is slow as evident from ground cracks and cracks in the walls on some of the buildings. It is difficult to monitor all of these landslides because of the steep Himalayan terrain and incoherent vegetation cover, including tea plantations. We focus our investigation on the Gayabari landslide (Figure 4) which is one of the many active landslides on these Himalayan slopes. The Gayabari landslide is a rockslide located on a moderately steep (25-35°) to steep (35-45°) slope at the right bank of Shiva Khola River. The landslide covers an area of 0.19 sq. km, and measures 647 m in length and 258 m in width. The only strategic railway (Darjeeling Himalayan Railway (DHR)), and National Highway (NH-55), connecting the scenic towns and tea plantations of Darjeeling Himalayas, run along the middle of the slide (Figure 4). The geomorphology of this terrain represents a complicated interaction of erosional and gravitational processes (mass wasting) which are sometimes triggered by active tectonic effects of the Himalayas and monsoonal heavy rainfall.

We used 20 RADARSAT-2 ultra-fine (3 m) scenes with downslope viewing acquired between September 2016 and January 2018. Five trihedral corner reflectors (CR) were installed to provide coherent signals for accurate time-series measurements. One CR was installed on a stable site away from the landslide. The measurement on the stable CR, shown in Figure 5, was compared with InSAR measurements taken from the active vegetated slopes. We used the GAMMA software to

generate unwrapped differential interferograms and used the SBAS method (Casu et al., 2006) to produce time-series displacement. We measured 2-5 cm motion over the year, with the maximum motion (shown in red in Figure 5) occurring during the wet monsoon season. The time-series displacement profiles for the CRs are also shown in Figure 5. The movement data from the pillars installed in and around the landslide area, as well as the prevalent ground cracks, coincide with the seasonal deformation measured from the InSAR analysis. Our study shows that InSAR can be used to develop an early warning system for monitoring active Himalayan landslides affecting critical infrastructure within the region.

2.5 InSAR deformation monitoring before and after Hurricane Maria, Dominica

Dominica is a small forested volcanic island (47 x 29 km) in the eastern Caribbean. Its highest peak is 1447 m asl, and about 60% of its slopes are steeper than 30% gradient (World Bank, 2004). Over 80% of the island is soaked by an average rainfall of 2500 mm throughout the year (Benson et al., 2001), especially in the hurricane season from June to November. The island's volcanic bedrock is overlain by weak wet clayey soils, which are prone to landslides, especially on steep slopes (De Graff, 2012). A national-scale landslide susceptibility map and research on triggering mechanisms for Dominica were conducted by van Westen (2016).

In September 2017, category 5 hurricane Maria triggered about 10,000 landslides throughout the island (van Westen and Zhang, 2017). It resulted in total damages of USD931 million, which amount to 226% of Dominica's 2016 gross domestic product (CDC, 2017). The need to reduce risk and build resilience for future hazards in Dominica was therefore identified (CDC, 2017). A community-based approach to landslide risk reduction to vulnerable communities has also been recommended (Anderson et al., 2011).

We used RADARSAT-2 InSAR to identify post landslide activity after hurricane Maria. We analysed 40 RADARSAT-2 multi-look fine (3 m) InSAR images from January 2014 to June 2018. Our results focused on bare slopes with good InSAR coherence and where landslides were expected to occur. Our results, for a small area in the eastern part of Dominica (Figure 6), is representative of the island. We show that there is considerable landslide motion on the crest of some of the bare slopes. Further work needs to be done because some bare slopes show landslide motion, but not all. We recommend more continuous rapid revisit InSAR monitoring throughout the year, especially during the hurricane season. This will assist in understanding the differential motion of the slopes within Dominica. This case study shows InSAR can be integrated with existing techniques to develop early warning and mitigation techniques for other hurricane prone Caribbean island states.

3: Energy Corridors

3.1 InSAR monitoring of pipeline routes

In Canada and elsewhere, discussions are ongoing regarding pipeline routing, monitoring, construction, and planning related to the distribution of oil and gas for processing and export. Detailed characterization of the terrain and ground movement along a pipeline corridor is critical for pipeline integrity (Porter et al., 2014). We provide three case studies using InSAR deformation time-series analysis as part of an early warning technique to monitor the safety of oil pipelines on different terrain. We analyzed 157 RADARSAT-2 InSAR images for the three sites discussed below. We focused on the use of InSAR to identify potential risks in the planning of pipeline routes within (1) a steep mountain valley and on (2) permafrost terrain. Our third case study used InSAR to monitor a pipeline built on a soft foundation within a wetland area where an oil spill has occurred. Our results show that InSAR deformation monitoring can be used to investigate areas of potential risk along pipeline routes.

3.2 Pipeline on Permafrost terrain

The study was conducted along the proposed Mackenzie Valley pipeline in northern Canada on permafrost terrain. The pipeline route was planned, many geotechnical studies conducted, but the pipeline was never built. Many important lessons were learnt however, related to large engineering projects planned on permafrost terrain. In addition, the socioeconomic impacts of permafrost degradation can be costly particularly for engineering construction in these areas (Larsen et al., 2008). This case study is only one example. Our objective here is to emphasize the importance of InSAR for monitoring current and planned infrastructure on permafrost terrain affected by its potential degradation.

Permafrost is defined as frozen ground that remains at or below 0 ^{o}C for two or more years. It is estimated to occupy about 24% of the northern hemisphere land surface (Zhang et al., 1999). The active layer of surficial material, approximately 1 m above the permafrost, freezes and thaws seasonally and therefore, affects the foundations of engineering and transportation infrastructures. Monitoring and mapping of recent permafrost degradation have been documented by Lawrence and Slater (2005), Lantuit and Pollard (2008), Short et al. (2011), Fraser et al. (2018), and others.

The Mackenzie Valley is experiencing one of the highest rises in mean annual temperature for any region in Canada. This increase in temperature is triggering climate driven thaw in the permafrost and subsequent landslides (Dyke and Brooks, 2000; Fraser et al., 2018). In areas where the thin forest cover is burned by wildfires, permafrost thaw and landslides are accelerated (Couture and Riopel, 2008). There are approximately 2,000 landslides, mainly triggered by climate driven permafrost thaw, along the proposed Mackenzie Valley pipeline route (Aylsworth et al., 2000).

This case study focuses on the Thunder River landslide within the pipeline corridor. The study area is characterized by permafrost with a thickness reaching up to 100 m. Relief is relatively low, with an elevation difference of 402 m. Vegetation cover is dominated by sparse-to-open coniferous forest, shrubs, and exposed land produced from natural fire scars.

The Thunder River landslide is a retrogressive thaw flow where the active layer is detached at the contact with the ground ice (Figure 7 insert). The slide debris consists of thawed permafrost with a slurry of sediments and melted water, which can flow at an angle as low as 1° to 2°. Such retrogressive thaw flows may start from a small-scale slope failure that can be as small as a few meters wide and retrogress over a distance as large as a few hundred meters (Wang et al., 2009). The deep thaw is caused by current warm summers combined with the destruction of the insulating surface from forest fires. The retrogressive failures may remain active for many years as long as the ice rich materials are exposed (Wang et al., 2009). Understanding the failure processes and their rates of movement are important in developing appropriate remedial measures related to the proposed Mackenzie Valley pipeline route.

Figure 7 shows typical ground motion from RADARSAT-2 and TerraSAR InSAR data during the summer months over permafrost terrain within the Thunder River area. Both InSAR observations presented similar temporal variations of deformation, with about 20 mm of downslope motion recorded from the corner reflectors installed near the retrogressive thaw flow landslide. However, TerraSAR provides more dynamic motion within the time-series because it has a shorter revisit time compared to RADARSAT-2. In Figure 8, the colours represent motion resulting from the active-layer freeze-thaw cycles, and warmer temperatures in the summer. The area in red shows small ground heave of about +20 mm and the areas in blue show thaw of about -20 mm over the summer months within the proposed pipeline corridor. Earlier long term InSAR monitoring studies using corner reflectors near the landslide (Figure 7) showed downslope motion of 20-30 cm from 2006-2010 (Singhroy, 2008; Singhroy et al., 2010). The maximum motion was observed during the summer months. The thin veneer of thermally-conductive mineral soils are linked to the active-layer responses to summer warming (Fraser et al., 2018). Farquharson et al. (2019) also reported ground subsidence totaling tens of centimeters within the active layer in some areas. Research on active layer response to summer warming is still ongoing as the responses are variable, and depend on a number of factors, such as local snow accumulation and active layer thickness (Zhang, 2005; Lawrence and Slater, 2010). To understand the impact of this dynamic motion on existing and future infrastructure, integrated monitoring would be required, including high-resolution rapid revisit InSAR provided by the RADARSAT Constellation Mission and other radar missions.

3.3 Pipeline routes in steep mountainous areas

This study focused on a proposed pipeline route within a narrow mountain valley in the Canadian Cordillera. The frequency of landslides on these mountain slopes are increasing and may be linked to climate change (Cloutier et al., 2017). The steep valley slopes produce debris flows which can affect pipeline routes. Identifying potential debris flows, and areas of downslope sediment accumulation is critical for pipeline safety within the valley.

InSAR monitoring was carried out following the methods outlined by Singhroy and Li (2017). We processed 17 RADARSAT-2 ultra-fine (3 m) scenes acquired from December 2015 to January 2017 in an area close to Nimbus Mountain, British Columbia, Canada. We selected a downslope view that corresponded to a slope angle of 35° in ascending orbit. We also selected short

perpendicular baselines (<100 m) with short time intervals between acquisitions, and corrected for topography and atmospheric conditions (Singhroy et al., 2012).

Our InSAR results show an area where debris flows occur. The area at Point 1 shows slope deformation at higher elevations in the debris flow channel. This corresponds to the area classified as having a high likelihood of landslide initiation in the geological map published by Maynard et al. (2018). Point 2 at the base of the slope is on a debris flow fan where sediment accumulation increases over time (Blais-Stevens et al., 2018; Figure 9). Furthermore, most of the steep stream channels also show sediment accumulation (blue) at their base. In the lower left area of Figure 9, the yellow indicates sediment depletion on the opposite side of the valley at high elevations. Identifying these areas of sediment motion in the upper and lower parts of the valley from InSAR data before a pipeline is constructed will assist in building safe pipelines and developing the appropriate mitigation measures.

3.4 Pipelines on wetland areas

Wetland areas are particularly challenging for pipeline construction. Seasonal displacement and swelling often cause structural damage to the pipes. The high compressibility of the peat results in consolidation, as well as lateral and horizontal displacement (Corrales et al., 2017). In the boreal forest regions of Canada, wetlands are also subjected to the freeze/thaw cycles. This seasonal process describes the transition of the landscape between frozen and thawed conditions which can be measured from ground reflected GNSS signals (Chew et al., 2017).

Our InSAR analysis over the wetland site uses nine years of RADARSAT-2 ultra-fine (134 images) data from August 2008 to November 2017. The resolution of the ultra-fine beam mode is ~1.6 m in range and ~2.8 m in azimuth. The InSAR processing was done using the same methods outlined by Singhroy and Li (2017). A 5 m resolution DEM was used for topographic correction. The flattened interferograms were filtered using an adaptive noise filter (Goldstein and Werner, 1998), unwrapped using a minimum-cost algorithm (Costantini, 1998) and geocoded (Pearse et al., 2014).

In July 2015, a pipeline spilled five million litres of emulsion (a mixture of bitumen, sand and water) at the Long Lake site in the oil sands region of northern Alberta (Singhroy et al., 2012). The spill occurred in the wetland area near the Steam Assisted Gravity Drainage (SAGD) site. Our nine year RADARSAT InSAR analysis (2008-2017) over this area shows a -10 cm deformation over the spill area (Figure 10). Investigation by the company suggests that the cause of the rupture was a thermally driven upheaval, along with an incompatible pipeline design for the muskeg ground conditions (Price, 2017). Our InSAR time-series results show seasonal fluctuations of 5 cm along the InSAR line of sight (LOS) before and after the oil spill within the wetland (muskeg) area. This amount of fluctuation can result in significant mechanical stress on the pipeline, and indicates that InSAR land motion monitoring on muskeg ground (and other wetland areas) is essential when developing an early warning system to prevent potential pipeline rupture.

4: Mining Infrastructure

4.1 InSAR monitoring of oil extraction in Alberta

Thermal viscous oil exploration requires a sound understanding of geomechanics to enhance the recovery process and reduce the environmental impacts. Surface deformation measurements, as part of the geomechanical monitoring process, are critically important. They provide a reliable way to calibrate and verify Thermal-Hydro-Mechanical (THM) models dealing with heat transfer, fluid flow, and mechanical stress and strain within a reservoir. The Alberta oil sands in northern Alberta contain one of the world's largest deposits of crude oil, in the form of viscous bitumen embedded within uncemented sand (Mossop, 1980; Mossop and Flach, 1983). The four major oil sand deposits extend over a large area of northern Alberta, with total initial in-place reserves estimated at about 1.8 trillion barrels (Oil Sands, 2010).

The oil sands differ from other crude oil deposits in that they are heavier and have a viscous tar-like consistency. They are unable to flow under reservoir conditions and must be recovered using unconventional methods. Mining reserves deeper than about 65 m is not economical. The bitumen must be produced in situ using enhanced recovery techniques. This relies on a thermal method of heating the bitumen to reduce its viscosity. This thermal method is known as the steam-assisted gravity drainage (SAGD) method. In the SAGD process, high-pressure steam is injected into the bitumen reservoirs at close to, or higher than, initial reservoir pressures. Groups of horizontal wells are drilled into the bitumen reservoir, side by side, while the heated oil drains from around the growing steam chambers, driven by gravity, to lower horizontal wells (Butler, 1994; Collins, 2007; Peacock, 2011). The combined withdrawal and injection of material into the subsurface is known to cause surface deformation, which has sometimes led to failure of well casings. The causes of failure depend on a variety of factors including the rate of the injection and withdrawal, temperature and pressure of injected material, properties of the reservoir and overburden, and local geology (ERCB, 2010; Peacock, 2011). We provide an example of InSAR monitoring of surface deformation at the Mackay SAGD site to identify and monitor potential over-pressure zones.

Glacial and recent deposits with different overburden and lithological thickness vary from 50 to 360 m above the bitumen productive layer. Singhroy et al. (2014) have shown that the overburden thickness is not influencing the surface heave. About 82% are considered to be recoverable mainly by thermal in situ methods and 18% by surface mining (Alberta Energy Utilities Board, 2005; Hein and Cotterill, 2006).

Several techniques are being used to measure surface deformation in the oil sands. These include levelling, gravimeters, tilt meters, inclinometers, GPS and InSAR (Stancliffe et al., 2001; Dusseault, 2011; Nur Khakin et al., 2013; Shen et al., 2014). We processed over 60 InSAR RADARSAT-2 ultra-fine mode (3 m) scenes starting from summer 2011 to fall 2013 at the Mackay site. Surface deformation is a response to changes in pressure and temperature in the subsurface,

so heave measurements can be used as a tool for monitoring reservoir pressures indirectly. The geomechanical process of SAGD, where constant pressure is used to achieve production through fluid gravity segregation, results in an increase in temperature, pressure, porosity, permeability, dilation and surface deformation (Dusseault, 2011; Shen et al., 2014). The InSAR observations show persistent surface heave occurring at rates of 2 cm/year over a two year monitoring period from 2011-2013 (Figure 11). We found that heaving above the horizontal injector wells is strongly correlated with rates of steam injection, even though there is a net fluid loss from the reservoir pore space as oil and water are withdrawn through the production wells. There are also minor swelling and ponding on the infill rehabilitation area near the tailings pond shown on (Figure 11).

4.2 Monitoring mining activities in Guyana

Mining in tropical countries significantly contributes to the global supply of minerals. Monitoring environmentally destructive illegal mining is a global problem, especially in the remote parts of South America and Africa (particularly Ghana and Congo) (Anser et al., 2014; Boadi et al., 2016). The practice of unregulated and illegal mining in these countries is sometimes associated with deforestation, loss of habitat and biodiversity, mercury pollution, and excessive river sediments. Small-scale gold mining in the remote, densely forested areas in the interior of Guyana are numerous, mobile and difficult to reach. It is estimated that the gold mining sector produces in excess of USD300 million in gold annually. The government is aware of the environmental problems produced by mining, but controlling them is beyond its capabilities (Roopernarine, 2014; Hilson and Laing, 2017). The majority of the country's gold mining is conducted by small and medium-scale operators. The mining properties of large international companies are known and regulated.

In this example, we used ALOS PALSAR (AP) imagery to monitor small-scale mining sites in one of the remote areas in Guyana. ALOS L-band images have been very useful for geological mapping in similar densely forested areas (Pour and Hasim, 2017). We focused our study on the use of change detection techniques applied to radar imagery to monitor small-scale gold mining activities along parts of the Mazaruni River in Guyana (Figures 12 & 13). The geometric and radiometrically corrected AP images were produced globally by JAXA for 2008 and 2016 (Global PALSAR-2/PALSAR/JERS-1 Mosaic and Forest/Non-Forest map https://www.eorc.jaxa.jp/ALOS/en/palsar_fnf/fnf_index.htm ; Singhroy et al., 2019). Based on the intensity level of the backscatter in the radar images, JAXA separated the data into three classes; water, forest, and non-forest. By identifying the areas that changed from forest in 2008 to non-forest in 2016, we were able to observe the changes in placer mining operations along rivers within this time period shown in yellow in Figure 12. Within the study area, our results show an increase of 370% in gold mining activities over this eight year period. The monitoring of mining activities of other areas can be done using this radar change detection technique. The change maps will assist these countries in monitoring legal and illegal mining activities.

4.3 Mineral exploration using radar image fusion

The search for minerals and engineering construction materials is an important part of mining infrastructure. In areas where the surficial materials and bedrock are covered by vegetation, there is a need to improve the interpretation of remote sensing images that indirectly provide useful

information on minable construction materials and minerals. Image enhancement and data fusion techniques have been used to facilitate the search for minable surficial materials and minerals in vegetated areas (Singhroy, 1996; Barnett et al., 2004; LaRocque et al., 2011; Harris et al., 2011, and others).

In this section, we present an example of using simple image fusion techniques to assist in delineating geological faults, as well as lithological contacts which are used in mineral exploration. Our example is focussed within an active mining area in Sudbury Canada.

The Sudbury impact structure is one of the world's largest producer of nickel. The area has about 90 Ni-Cu-PGE (nickel, copper, platinum-group metals) deposits, and includes several operating mines. The mineralization is mainly associated with the basal contact of the Sudbury Igneous Complex (SIG) (Ames et al., 2008). Norite and gabbro are two of the four major lithologies of the SIG shown in Figure 14. Tuba et al. (2014), and others, have suggested that large-scale brittle fault structures are conduits for PGE enriched fluids in Sudbury and several other locations around the world. Mapping the surface expression of faults using radar images has been extensively reported by Lowman (1991), Singhroy et al. (1993), Singhroy and Lowman (2012), and others.

The Sudbury area consists of glaciated undulating terrain (400 m) covered by trees within the boreal forest. Unlike images/air photos from which topographic maps are produced, or a lidar image which looks down perpendicular at the terrain, we selected a 35° viewing angle to enhance topographically controlled structures. In addition, we added three different polarizations of RADARSAT-2 imagery (VH, HH, and VV) to enhance the moisture captured in the faults (Figure 14). Radar is a moisture seeker, and recent research has shown (Fobert et al., 2018) that polarimetric radar imagery are particularly useful in mapping moisture trapped faults in vegetated terrains. Optical satellite images such as Landsat are less useful because their optical and infrared bands are not as sensitive to moisture filled linear features as the SAR backscatter.

Using the biased viewing angle and the polarimetric radar images we provide an example where a polarimetric composite image (Figure 14 c) provides additional information on lithologic contacts and faults to assist in mineral exploration programs. The fusion of radar and airborne magnetic images (Figure 14 a) have enhanced the interpretation of the magnetic images by confirming the magnetic signatures related to faults, dykes or contacts, and add new topographically expressed or moisture filled faults. Figure 14b shows an example where there is a need to update an existing geological map. The radar image overlay can also confirm or add lithological and structural information. These integrated radar image maps provide additional and up-to-date structural and lithologic contact information to assist in targeting drilling areas for exploration, education, and research.

5: Coastal Infrastructure

5.1 Monitoring coastal change using radar time series images

Coastal areas are the most vulnerable to climate change due to sea level rise (SLR). This includes coastal flooding and changes to the littoral processes (i.e., sediment transport patterns) (Nicholls et al., 2011; Sánchez-Arcilla et al., 2011).

All of the productive agricultural lands, and most of Guyana's population, reside in the narrow and fertile coastal plain (425 × 50 km), which is below sea level. The coastal dikes, and concrete and earth dams constructed for sea defence, need constant monitoring and improvement to control flooding, and to protect both coastal infrastructure settlements and irrigation for agricultural areas.

This study shows that parts of the Guyana coastline are undergoing significant changes. Recent research has shown that changes of a few meters to half of a kilometer have occurred from satellite image observations over the past 50 years (Singhroy, 1996a 1999). Similar coastline changes observed from radar imagery are occurring along the coast of French Guyana and NE Brazil (Barbosa et al., 1999; Trebossen et al., 2005). This rate of change is variable and occurred on different parts of the coastline. The changes are due to SLR, sand mining, mangrove depletion, and natural shoreline erosion and accretion processes (Singhroy 1995, 1997; Temitope et al., 2019). Ahmad (2012) utilized a Geographical Information System (GIS)-based approach to model coastline changes, i.e., its linkages to recurring episodes of coastal accretion, erosion, and mud bank development.

An example of shoreline change is shown in Figure 15. We observe a change of 0-400 m from 2007-2018 using ALOS L-band radar imagery. The results show areas of stable, eroded, and accreted shoreline. There appears to be more areas of erosion than accretion which may be the result of increasing storm events due to SLR. Our example is a snapshot of similar processes that are occurring along the entire Guyana coastline. This has serious implications for sea defence, mangrove protection and restoration, and flood protection for infrastructure settlements and agriculture. Measuring the shoreline changes from satellite radar imagery will also assist in locating areas for near-shore gas pipeline facilities being planned because of the recent offshore oil and gas discoveries. In addition, the potential of oil spills along the Guyana coast requires the need to understand the dynamics of long and short term littoral processes, and requires the ability to monitor and measure the impacts of oil spills on coastal ecosystems.

5.2 Oil spill monitoring

Ocean oil spills can be caused by tanker ruptures, illegal oil discharges by ships, or natural oil seepage. The International Tanker Owners Pollution Federation (ITOPF) estimated that between 1970 and 2016 approximately 5.73 million tons of oil were lost as a result of tanker incidents (Roser, 2020). However, these incidents have decreased substantially since 1970. While the majority of these spills are minor (less than 7 tons) (ITOPF), both large and small spills can cause serious damage to coastal ecosystems and can harm coastlines and near-shore waters.

Radar imagery is highly useful in the detection of oil spills because of its day and night imagining capability and the clear distinction of oil on the sea surface. Oil spills floating on the sea surface appear dark on the radar image (Figure 16). The oil slicks dampen the surface waves resulting in a low radar backscatter (dark areas). However, not all dark areas on the ocean surface are oil spills. The dark areas on the open ocean surface can sometimes have lookalikes. These include cold water upwelling, flow regimes associated with internal waves and oceanic eddies, changes in the stability of the air-sea interface, and from natural surface films produced by large areas of plankton or fish (Alpers et al., 2017). Manual and automatic pattern recognition techniques are used to discriminate between oil slicks and lookalikes (Brekkea and Solbergb, 2005; Alpers et al., 2017). In addition, polarimetric SAR observations have been used to improve the oil slick characterization and separation from lookalikes (Migliaccio et al., 2015).

In this case study, we report on a recent oil spill off the coast of Newfoundland, Canada and the use of RADARSAT imagery to discriminate the spill. On July 17th, 2019, approximately 12,000 litres of oil and water leaked from a storage tank aboard the Hibernia offshore oil platform (C-NLOPB, 2019). The data used were RADARSAT-2 Standard mode 5 acquired on July 21st, 2019. The polarization selected was VV as it is well suited for marine applications such as oil spill detection (Li et al., 2018). The data were obtained in an ascending right-looking orbit, with incidence angles of 36^{o} to 42^{o} and 12.5 x 12.5 m spatial resolution. Subsequently, the data were geometrically corrected and filtered with a 5 x 5 Enhanced Lee filter (Hu et al., 2012). Normalization was then applied to enhance visualization.

Our results show that the oil spills appear dark on the image. This was a relatively calm sea and as such the separation of the oil slicks from the background ocean was very clear (Figure 16). The oil platforms act as corner reflectors and appear as bright targets on the image. There were no cleanup efforts for this particular spill because the oil was very thin and therefore not suitable for cleanup.

Although oil spills can be easily detected during relatively calm ocean conditions, continuing research and verification methods are being developed for the estimation of oil spill thickness, and on the discrimination of oil spills from lookalikes (Fingas, 2018).

6: Conclusion

We provided a review on the application potential of the common sensors that are being used for monitoring infrastructure. We focussed on case studies using high-resolution radar and InSAR images for critical transportation and energy corridors, mining, and coastal infrastructure. These case studies will assist in developing integrated early warning systems and mitigation strategies for climate resilient infrastructure.

Our case studies show that:

- High-resolution InSAR images are effective in monitoring landslides along highways and railways in coastal and mountainous Himalayan communities. Land motion is triggered during active wet spring periods (Newfoundland and Quebec), monsoons (Indian Himalayan), and the

hurricane season (Dominica). Landslides are spontaneous and require timely InSAR images from the RADARSAT Constellation Mission (4 days), and other radar constellations. In the tropical island states, and on steep Himalayan slopes, more rapid InSAR monitoring is needed during hurricane, typhoon and monsoon events.

- As part of safe mining practices, InSAR is used to monitor uplift rates produced by steam injection in the mining of the oil sands in Canada. The surface heaving measurements will assist in understanding the dynamic changes of the reservoir properties.
- InSAR is used to monitor pipeline corridors in high risk mountainous, wetland, and permafrost terrain. This can assist in targeting geotechnical investigations and develop an early warning system to prevent potential oil spills.
- Change detection techniques of multi-temporal radar images are effective in monitoring mining infrastructures in remote vegetated tropical areas. This can help in identifying illegal mining in cloudy remote tropical areas.
- Coastal erosion and accretion change low lying shorelines. Radar time-series and change detection techniques are useful to monitor these shifting coastlines. This is significant for monitoring the effects of the rising sea level on low lying coastlines and nearby coastal infrastructure.
- The fusion of high-resolution vertical gradient magnetics and multipolarization radar images is providing additional information for the improvement of fault and rock unit delineation in vegetated areas. This will assist in mineral exploration.
- Radar images are very useful in detecting oil spills in the ocean. Research is currently ongoing to differentiate oil spills from lookalikes.

Acknowledgements

The case studies described above are an extension and a reinterpretation of the published works conducted by the authors at the Canada Centre for Remote Sensing. The methodologies are simplified for a general audience.

References
(See Springer Book for complete paper)

Table 1. Current and Planned Radar Satellites 2007-2025

Satellite	Radarsat-2	Radarsat Constellation Mission (RCM)	TerraSAR-X (TSX)	TanDEM-X (TDX)	ALOS-2/ALOS-4	Cosmo/ Skymed	Sentinel-1A/ -1 B
Space Agency	CSA	CSA	DLR	DLR	JAXA	ASI	ESA
Launch	2007	2019	2007	2010	2014/ 2020	2007 – 2010	2014/2016
Band	C	C	X	X	L	X	C
Wavelength (cm)	5.7	5.7	3.1	3.1	22.9	3.1	5.6
Polarization	Single, Dual, Quad	Single, Dual, Quad, CP	Single, Dual, Quad	Single, Dual, Quad	Single, Dual, Quad, (experimental CP)	Single, Dual	HH, Dual
Incidence Angle (deg)	10-60	10-60	15-60	20-55	8-70	Variable	20-46
Resolution Range (m)	3-100	1-100	1-16	1-16	3-100	1-100	2-93
Resolution Azimuth (m)	3-100	3-100	1-16	1-16	1-100	1-100	5-89
Scene Width (km)	50-500	5-500	5-100	5-100	25-490	10-200 (up to 1300)	20-410
Repeat Cycle (days) InSAR	24	4-12	2-11	2-11	14	5-16	12
Orbital Elevation (km)	798	592	514	515	628	620	693

Table 1 (continued). Current and Planned Radar Satellites 2007-2025

Satellite	NISAR	Capella X-SAR Constellation	ICEYE Constellation	KOMPSAT 5/6	NovaSAR-1	PAZ (aka SEOSAR)
Space Agency	NASA/ ISRO	Palo Alto	ICEYE	KARI	UKSA	HISDESAT
Launch	2022	2018 - 2021	2018 - 2020	2013/2025	2018	2018
Band	L, S	X	X	X	S	X
Wavelength (cm)	24, 12	3.1	3.1	3.2	10	3.1
Polarization	All	HH	VV	Single	Single, Dual, Tri (HH+VV+HV)	Single, Dual
Incidence Angle (deg)	33-47	10 – 50	10-35	20 - 55	16 - 73	15 - 60
Resolution Range (m)	3 - 48, 3 - 24	0.3 - 10	1 - 20	1 - 20	6 - 35	1 - 6
Resolution Azimuth (m)	7	0.3 - 1	1 - 20	1 - 20	6 - 35	1 - 16
Scene Width (km)	> 240	10 - 50	5 - 30	5 - 100	20 - 400	5 - 100
Repeat Cycle (days)	12	0.13 - 0.25 (3 - 6 hours)	1	28	16	11
Orbital Elevation (km)	747	485 - 525	570	550	583	514

Table 2. Application potential of RADARSAT-1, RADARSAT-2[1], and RCM. Key:'1' use of single data images assumed, '-' minimal, '-/+' limited, '+' moderate, '++' strong, 'CP' compact pol, 'P' polarimetric. van der Sanden (2004) modified by Singhroy.

		Satellite		
	Application	RADARSAT-1	RADARSAT-2	RCM
Agriculture	Crop type	-/+	++P	++CP
	Crop condition	-/+	++P	++CP
	Crop yield	-	-/+	-/+
Cartography	DEM interferometry	+	+	++
	DEM stereoscopy	++	++	++
	DEM polarimetry	N.A.	-/+	-
	Cartographic feature extraction	+	++	++
Disaster Management	Floods	++	++	++
	Geological hazards	-/+	++	++
	Hurricanes	+	+	+
	Oil spills	++	++	++
	Search and rescue	-/+	+	+
Forestry	Forest type	-/+	-/+	+
	Clearcuts	-/+	++	++
	Fire-scars	-/+	++	++
	Biomass	-	-/+	-/+
Geology	Terrain mapping	-/+	+	+
	Structure	++	++	++CP
	Lithology	-/+	-/+	-/+
Hydrology	Soil moisture	-/+	+	+CP
	Snow	-/+	+	+
	Wetlands	-/+	++	++CP
Oceans	Winds	+	++	++
	Ships	+	++	++CP
	Waves	-/+	-/+	+
	Currents	-/+	+	+
	Coastal zones	-/+	++	++
Sea and Land Ice	River Ice	+	++	++
	Sea ice edge and ice concentration	+	++	++CP
	Sea ice type	+	++	++CP
	Sea ice topography and structure	-/+	++	++CP
	Icebergs	-/+	++	++
	Polar glaciology	-/+	++	++
InSAR Motion Applications	Subsidence		++	++
	Slope Stability/Landslides		++	++
	Co-seismic Deformation		++	++
	Oil Sands Mine Heaving		++	++
	Land Motion		++	++

Table 3. Potential application of advanced remote sensing for infrastructure. Key: '-' minimal, '-/+' limited, '+' moderate, and '++' strong.

Application	Stereo Air photos	Drone	Lidar	High-Resolution Optical	Radar	InSAR Land Motion
Buildings Urban/Rural	++	++	++	++	+	++
Transportation Corridor Roads/Highways, Railway	++	++	++	++	+	++
Dykes/Dams	+	++	++	++	+	++
Mine Wall Motion	-	+	+	-	-	++
Flood Extent	++	++	+	+	++	-
Damaged Buildings	++	++	+	++	++	
Bridge Motion	-	-	-	-	++	++
Fire Damage	++	++	-	++	+	-
Land Motion	++	++	+	++	+	++
Construction Materials Metals (Mining) Geological Structures	++	-	+	+	++	-

List of Figures

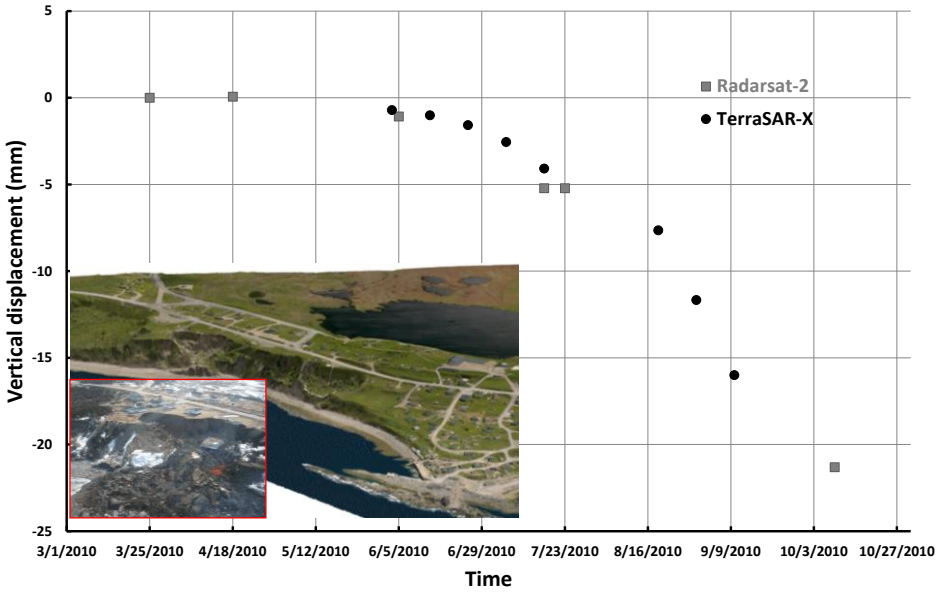

Figure 1: InSAR motion at Daniel's Harbour.

Figure 2: Two metallic trihedrals installed on the retaining wall along the railway (1&2) and one on the tilted block (3). Reflector 1 shows a differential GPS instrument which provided measurements to validate the InSAR results.

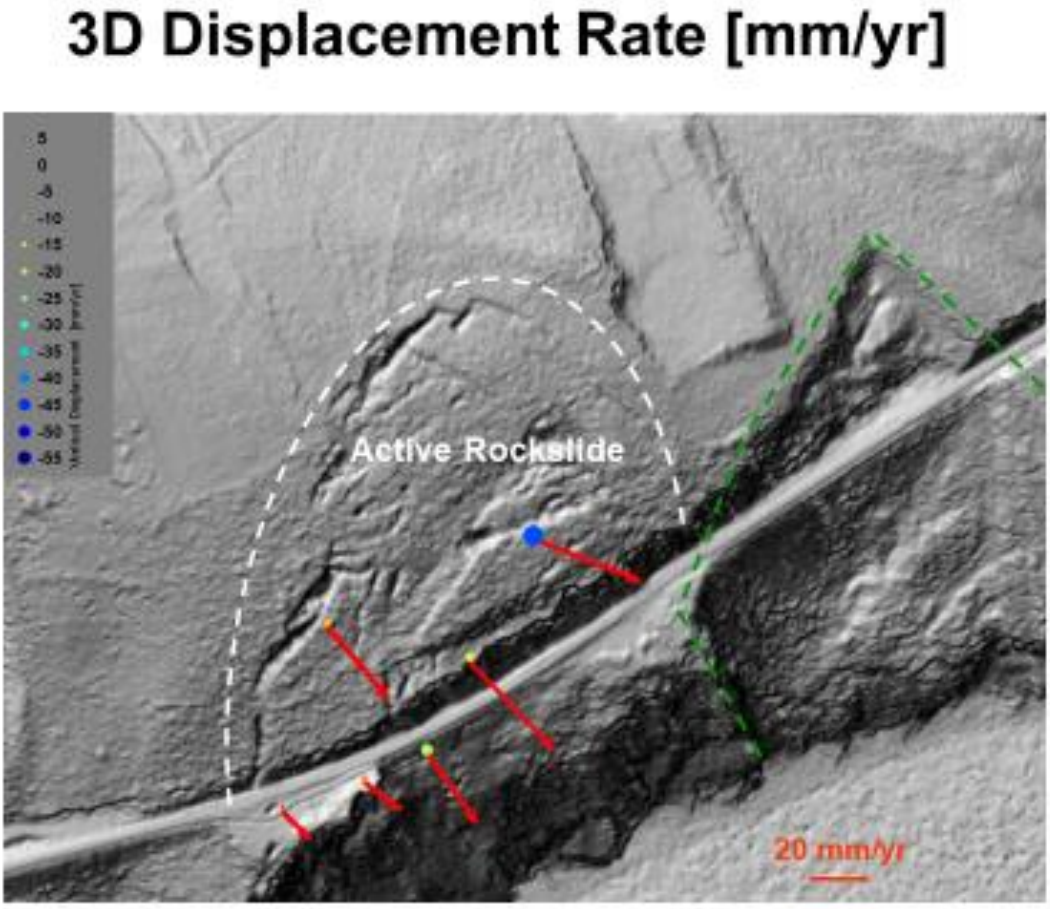

Figure 3: RADARSAT InSAR results showing rockslide motion at the Gascons Landslide, Quebec. The LIDAR image shows the outline (white stippled line) of the rockslide and the railway line. Red arrows shows displacement (direction and annual horizontal rate) of the different rockslide blocks. The colored circles indicate reflector location and their vertical displacement rate. Locations with ascending and descending configurations are shown.

Figure 4: View of the Gayabari Landslide. The Giddapahar village is situated just above the crown of the landslide. The Darjeeling Himalaya Railway (DHR)/ NH-55 connecting Darjeeling district passes through the middle of the Gayabari landslide.

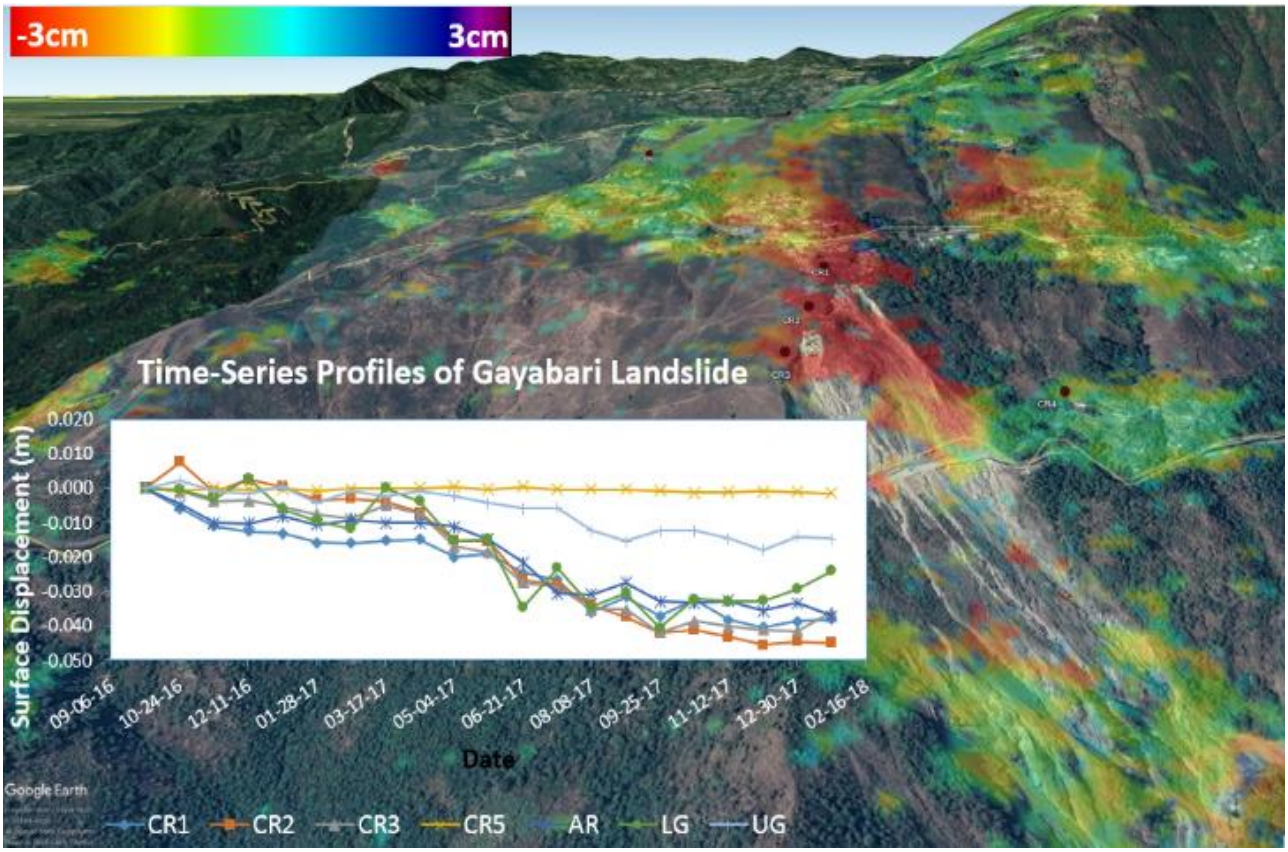

Figure 5: Gayabari landslide displacement motion from RADARSAT-2 InSAR. The black dots on the image show the location of the installed corner reflectors (CRs).

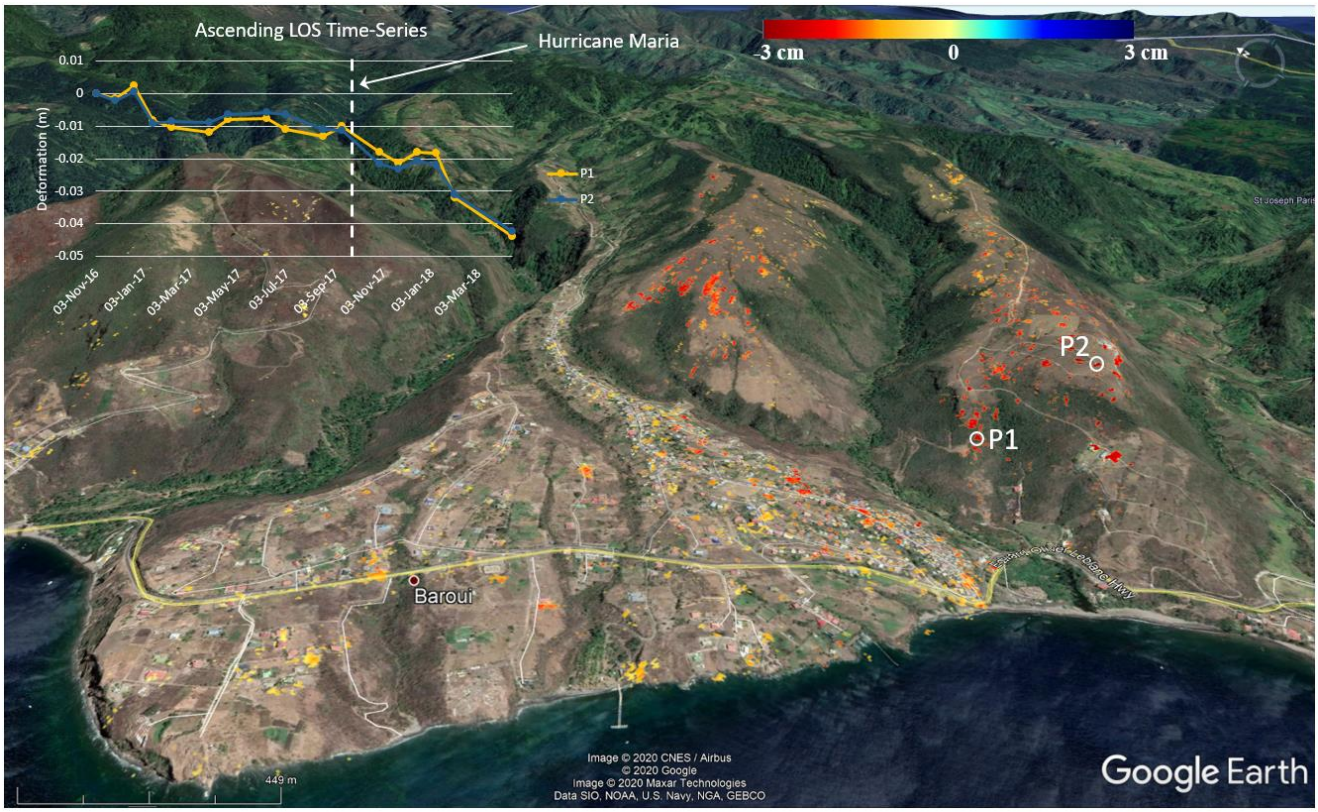

Figure 6: Landslide motion from RADARSAT-2 InSAR over Dominica before and after Hurricane Maria (September 2017).

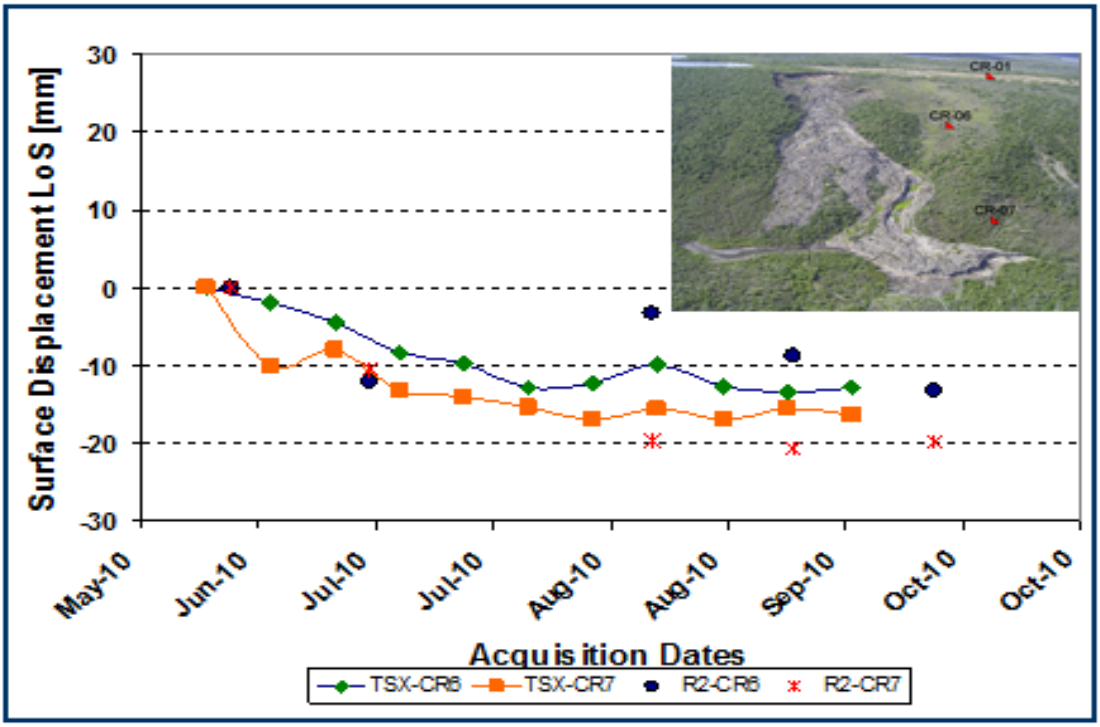

Figure 7: RADARSAT 2 and TerraSAR InSAR time-series showing surface deformation resulting from permafrost thaw within the active-layer due to warmer summer temperatures at the Thunder River landslide.

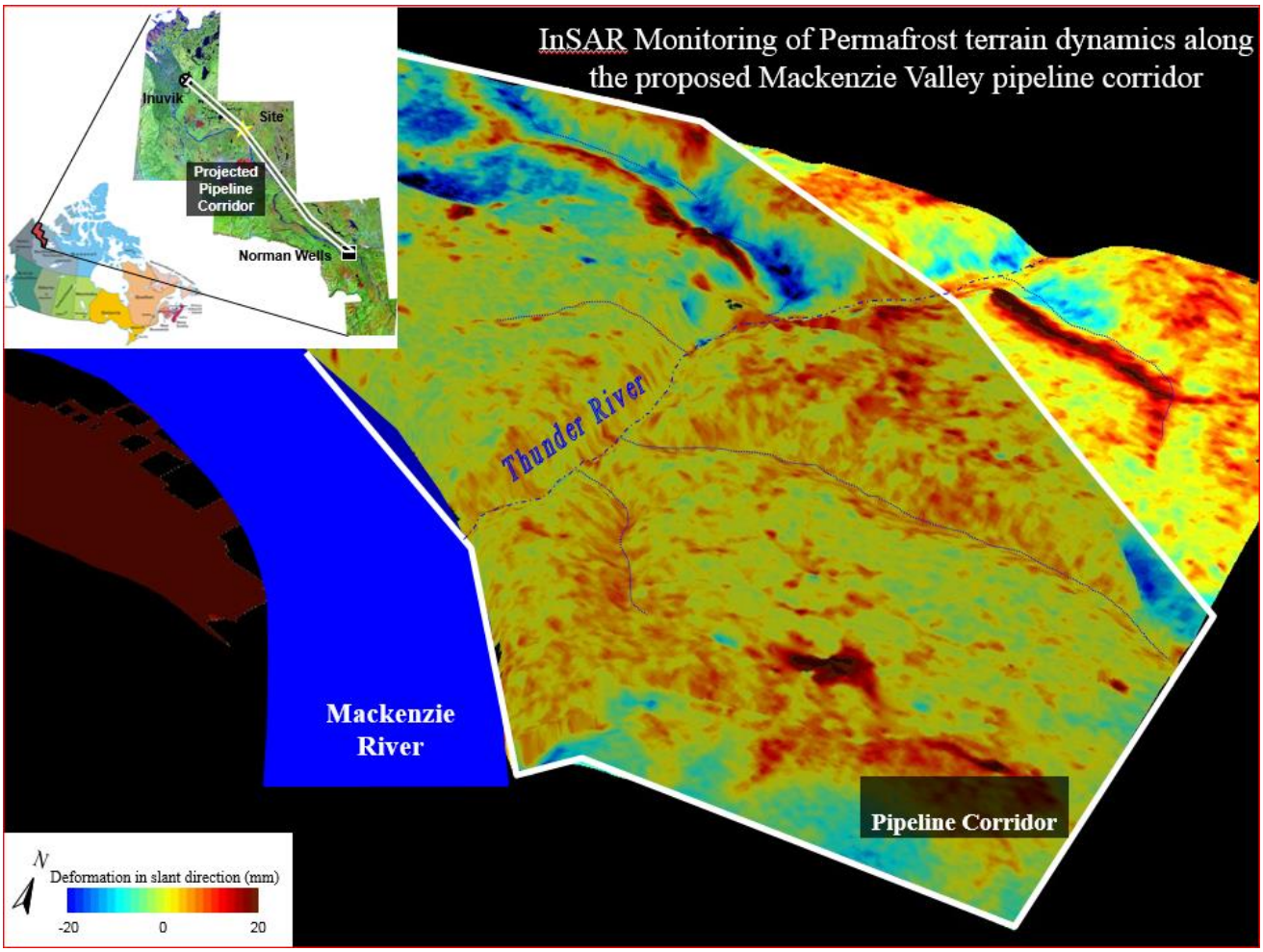

Figure 8: InSAR deformation monitoring on a proposed pipeline route over permafrost terrain. Red areas show where the ground is heaving (swells) and the blue areas show where the ground is sinking because of thawing.

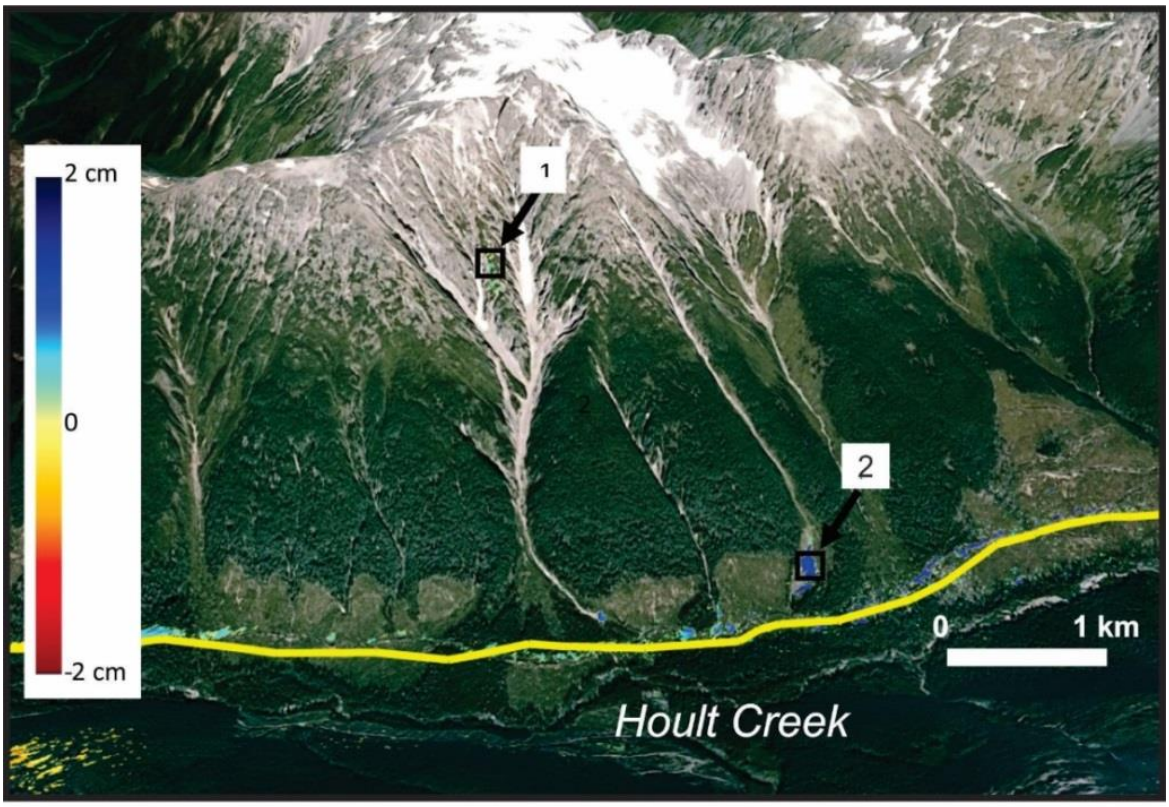

Figure 9: Ground displacement results from InSAR monitoring of slopes within the Holt Creek valley. Blue tones indicate accumulation of sediment and yellow and red tones indicate depletion and potential debris flow zones. Points 1 and 2 reflect active debris flow channels. The yellow line shows a previously proposed pipeline route (Blais-Stevens et al. 2018).

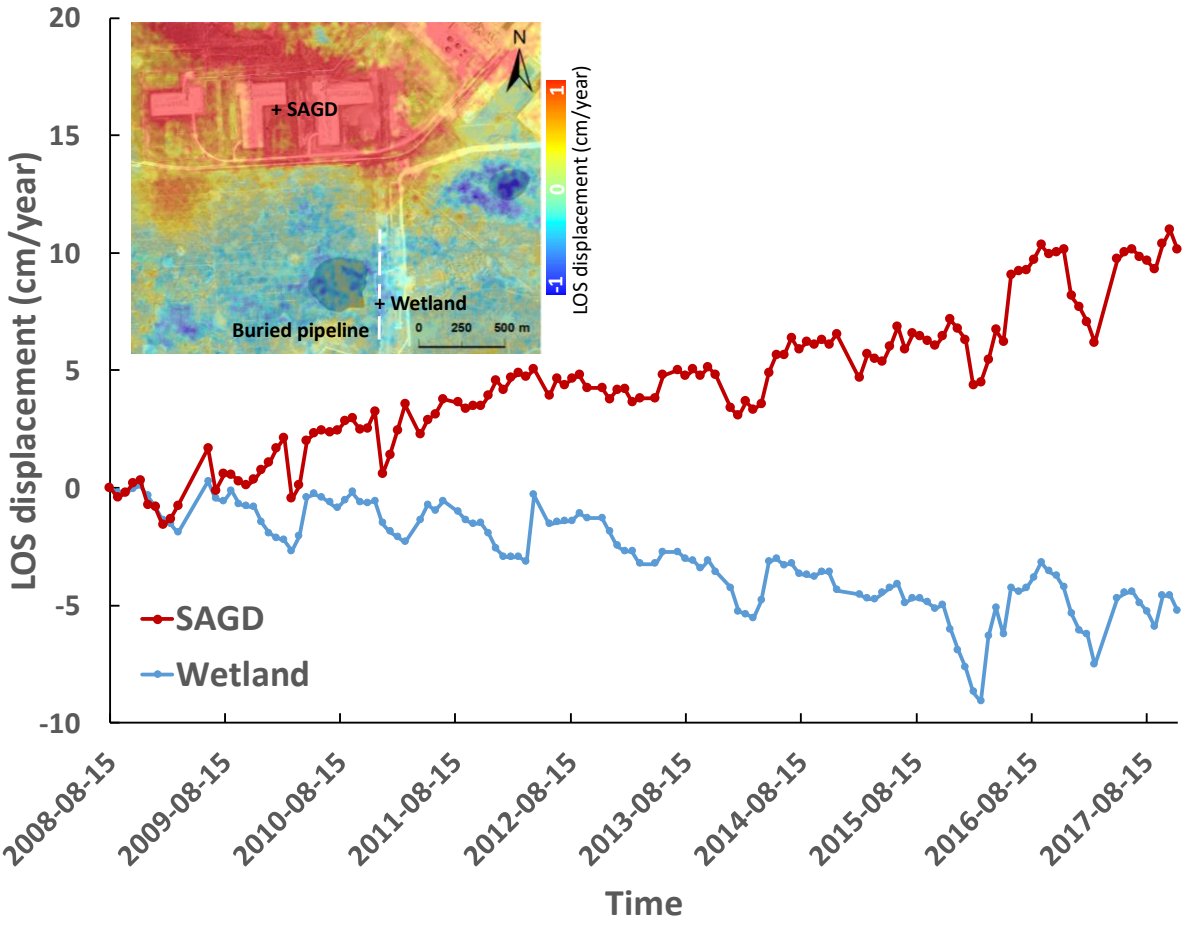

Figure 10: InSAR deformation due to a pipeline leak on a wetland (blue) near SAGD site (Red) using RADARSAT InSAR time-series.

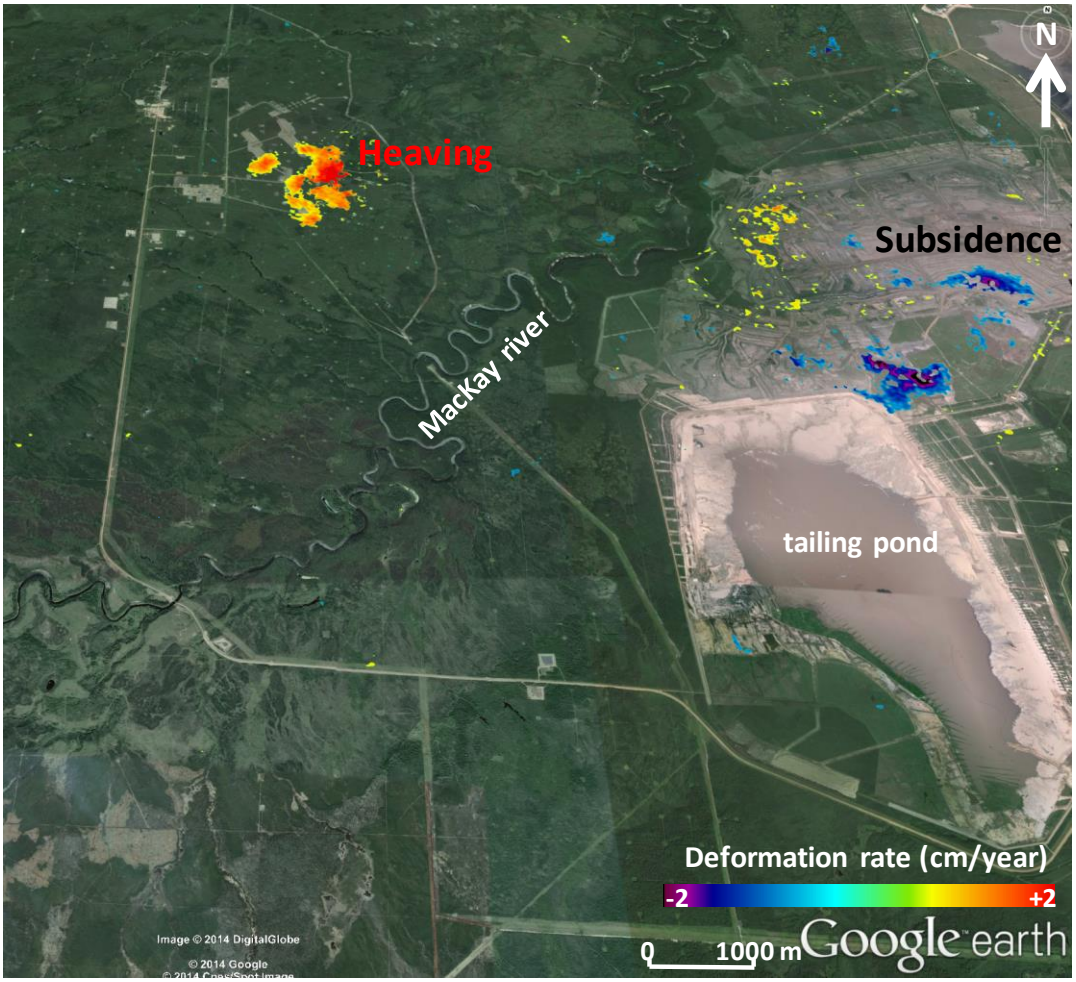

Figure 11: RADARSAT-2 InSAR time-series showing surface deformation at the Mackay River SAGD extraction site.

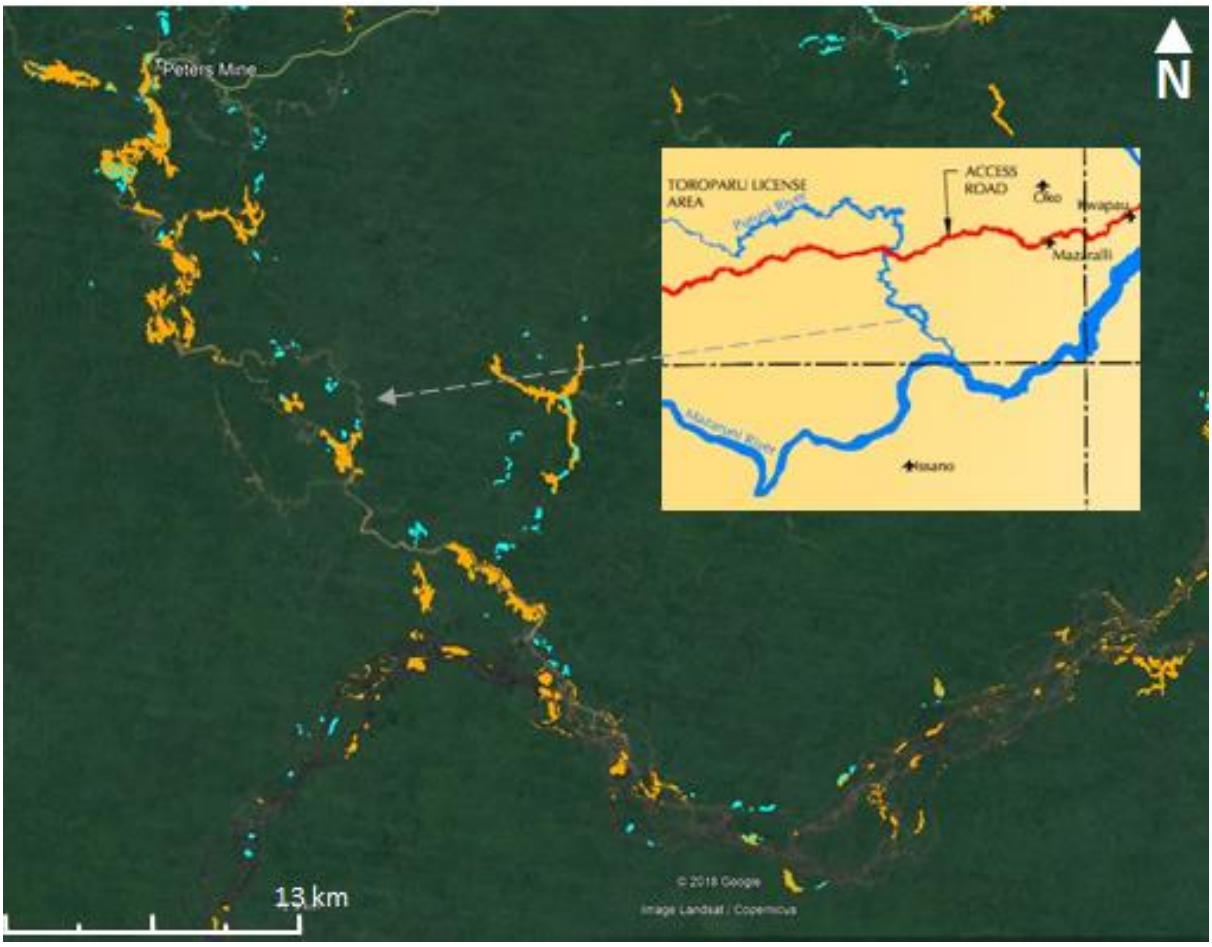

Figure 12: Placer gold mining along river banks in a cloudy, dense tropical forest identified from ALOS PALSAR images. The yellow colour represents the changes in mining operations from 2008-16. Comparing these areas with registered mining leases will help identify illegal mining opperations. Inset map helps to identify the location of the small scale mining.

Figure 13: Field photo of local small scale unregulated placer gold mining in the tropical forest areas in Guyana (Guyana Geology and Mines, 2019).

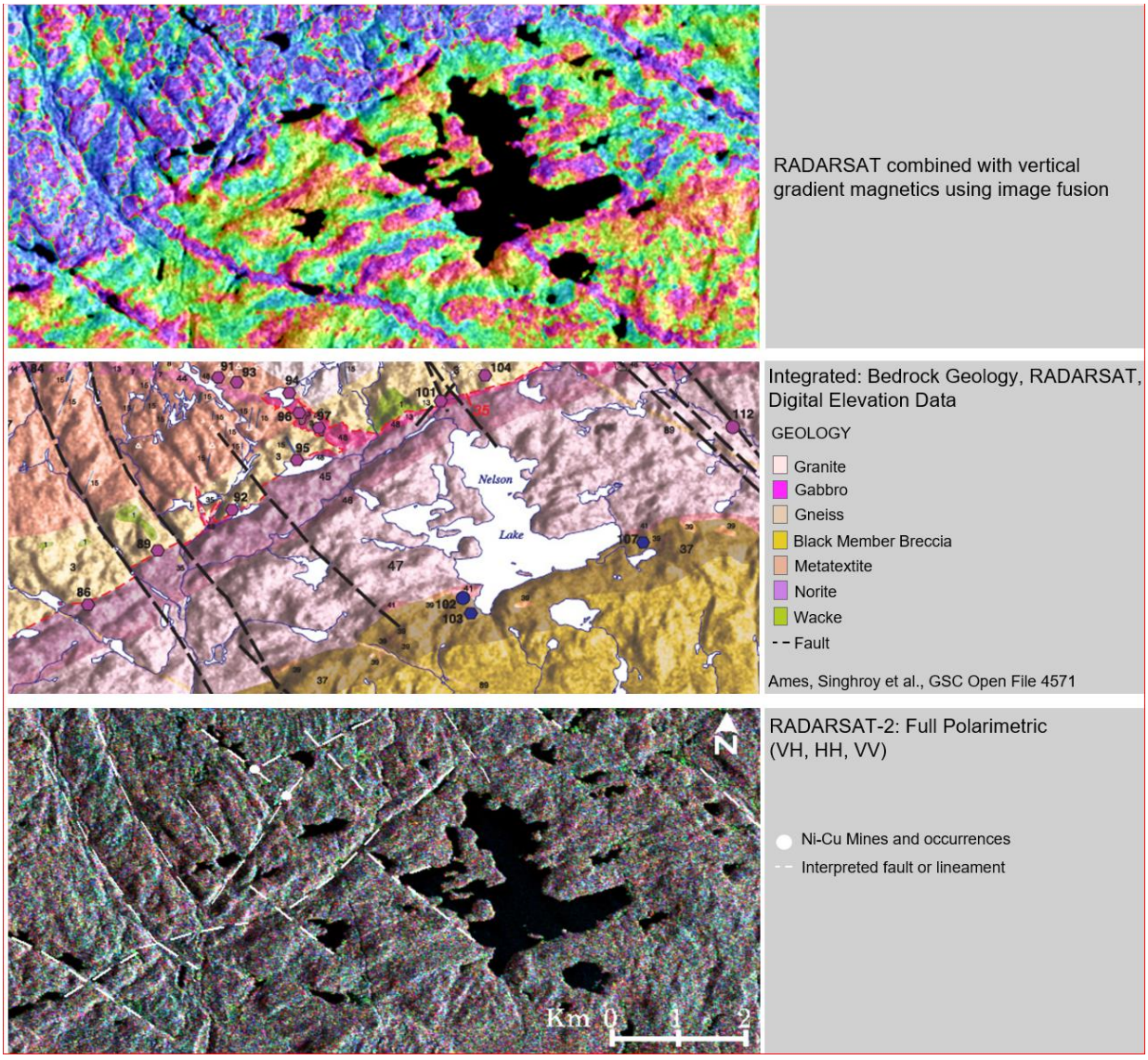

Figure 14: shows image fusion techniques used to identify faults, rock types, and contact zones which control the nickel copper (Ni Cu) mineralization (Ames et al., 2006) in the Nelson Lake area, Sudbury, Ontario. (a) shows the fusion of vertical gradient magnetics and a RADARSAT image. Faults are shown as NW-SE red linears. (b) shows the published rock types, faults and mineral map overlain on a RADARSAT image. (c) shows a polarimetric RADARSAT-2 image (VH, HH, VV) used to identify additional NW-SE faults and SW-NE contacts not clearly shown on the geological map and magnetic image.

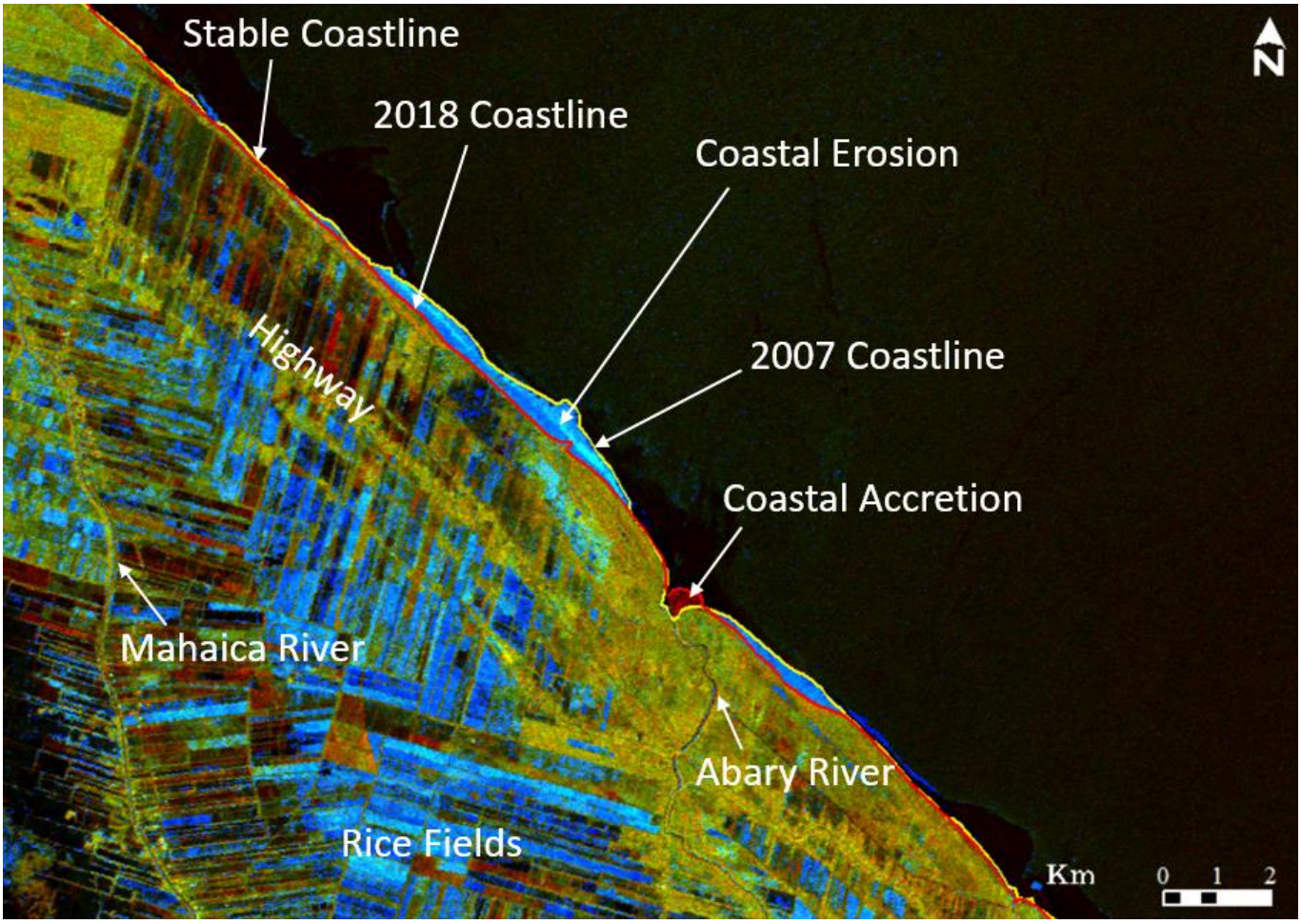

Figure 15: Coastal changes of the Guyana coastline over an 11 year period (2007-2018) using cloud free radar images.

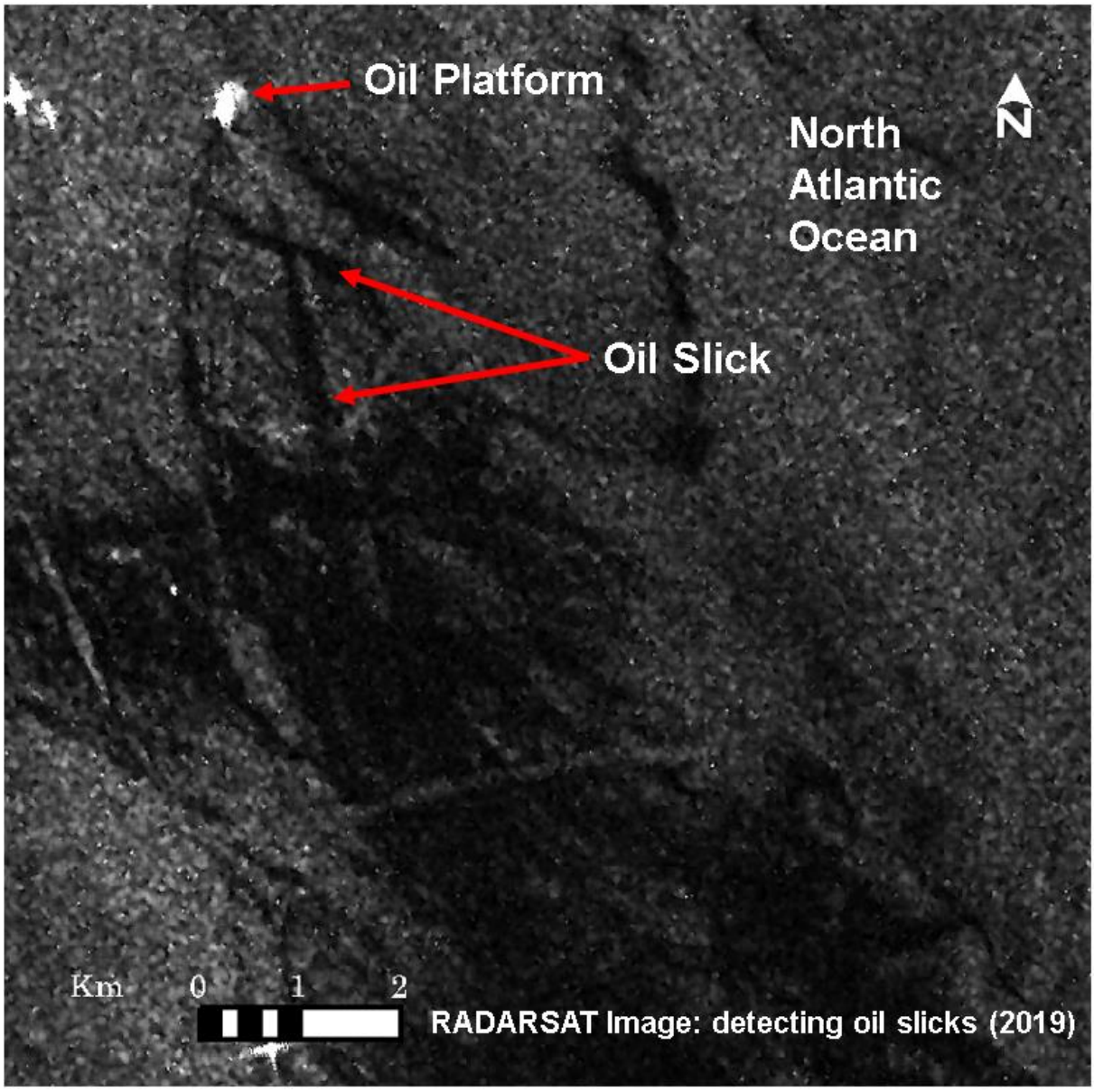

Figure 16: RADARSAT-2 image showing the extent of the oil spill from July 2019 (dark areas) near the Hibernia oil platform in the North Atlantic (2019).